Journal of Power Sources 196 (2011) 10249–10253

Contents lists available at ScienceDirect

Journal of Power Sources

journal homepage: www.elsevier.com/locate/jpowsour

Short communication

Electrochemical performances of graphene nanosheets prepared through microwave radiation

A.M. Shanmugharaj, W.S. Choi, C.W. Lee, Sung Hun Ryu*

Department of Chemical Engineering, College of Engineering, Kyung Hee University, Yongin, Kyunggi-Do 449701, South Korea

ARTICLE INFO

Article history:
Received 26 May 2011
Received in revised form 28 June 2011
Accepted 5 August 2011
Available online 12 August 2011

Keywords:
Graphene
Lithium ion battery
Anode materials
Microwave radiation
Discharge capacity

ABSTRACT

Graphene nanosheets (GNSs) are prepared by oxidation and rapid expansion of graphite using microwave radiation. The prepared GNSs are characterized using various characterization tools. Morphological characterization using field emission scanning electron microscopy (FE-SEM) and transmission electron microscopic (TEM) studies revealed that the GNSs prepared through microwave radiation are crumbled with scrolled and entangled nature. Raman spectroscopy and X-ray diffraction (XRD) studies confirmed the graphitic crystalline structure of the synthesized GNSs. The surface composition and functional groups introduced on the surface of GNSs due to microwave radiation are corroborated using X-ray photoelectron spectroscopy (XPS) and Fourier transform Infrared Spectroscopy (FT-IR). Electrochemical characterization studies of GNSs based anode materials showed an enhanced lithium storage capacity and fine cycle performance. The initial discharge capacity of GNS electrode is 580 mAh g^{-1} that decreases to 420 mAh g^{-1} at 50th cycle. Electrochemical impedance spectral analysis reveals that the exchange current density of GNSs increases with the charge–discharge cycle numbers exhibiting the peculiar electrochemical performance.

1. Introduction

Nowadays, Li ion batteries are being considered for various ranges of applications, including portable electronics and high power hybrid vehicles due to their high volumetric and gravimetric energy densities compared to that of other known secondary batteries. One of the major challenges for designing electrodes for lithium ion batteries (LIB) is to make a material with high Li storage capacity and columbic efficiency (that is, a high ratio of extractable lithium to inserted lithium) [1]. Significant research has been done to enhance the specific capacity as well as cyclic performance of the lithium ion batteries [1,2]. Graphite is widely used as anode material in lithium ion batteries owing to its high columbic efficiency and acceptable specific capacity by forming intercalation compounds (LiC_6) [3]. Research attempts have been made to enhance reversible capacity of the graphite electrode by introducing defects, channels and functional groups on the surface [4–8,9].

The discovery of nanocrystalline graphene thin films motivated the researchers to carry out basic research to understand the electronic and mechanical properties of the graphene sheets [10–12]. Extensive research has been carried out on the electrochemical performances of the graphene-based anode materials due to their high conductivity, large surface area and good mechanical properties that are comparable with, or better than, those of the carbon nanotubes [13–16]. Prior to the research report on the graphene-based anode materials, Fukuda et al. [17] reported the electrochemical properties of the foliated natural graphite as the anode material for LIB, and they reported that by applying chemical flaking of the natural graphite, it can be possible to obtain electrodes with the specific rechargeable capacities that are close to the theoretical value of 372 mAh g^{-1}. Recently, Yoo et al. [18] investigated the possibility of higher lithium storage capacity by controlling layered structures of the graphene nanosheet materials. They observed the reversible capacities increased to about 800 mAh g^{-1}, when the graphene layer-to-layer distance was increased by introducing nanotubes and fullerenes between the layers. Larger interlayer distance of the few-layered graphene nanosheets plays a vital role in increasing the capacity compared to the pristine graphite [19]. Dahn et al. [20] proposed that the graphenes in disordered carbons should have a higher reversible capacity since both sides of the graphene could host lithium ions. Therefore, the graphene nanosheets comprising of many disorganized graphenes would exhibit potential application when used as anode material for LIB.

Graphene nanosheets used for fabrication of lithium ion anode materials were mostly synthesized through physical, electrochemical or chemical methods in which individual graphene layers were

* Corresponding author. Tel.: +82 31 201 2534; fax: +82 31 202 1946.
E-mail address: shryu@khu.ac.kr (S.H. Ryu).

0378-7753/$ – see front matter © 2011 Elsevier B.V. All rights reserved.
doi:10.1016/j.jpowsour.2011.08.039

extracted from graphite, carbon fibers or carbon nanotubes [21]. Most of the chemical methods reported till dates rely heavily on the usage of harsh oxidizers like $H_2SO_4/KMnO_4$ [21], carboxylic acid [22] or formic acid [23]. Recently, synthesis of graphene has been done through eco-friendly route using microwave radiation [24]. Though graphene synthesized through eco-friendly route received a lot of attention because of their unique properties, they have never been studied as an electrode material for Li-ion batteries.

In the present study, for the first time, we investigated the electrochemical properties of Graphene nanosheets prepared through microwave-assisted eco-friendly synthesis route so as to understand the lithium storage properties of these novel graphene materials. Results obtained from various electrochemical techniques like cyclic voltammetry, electrochemical impedance spectroscopy and battery analyzer are being described.

2. Experimental

GNSs were prepared by taking 2:0.1:2 weight ratio of Natural graphite (Sigma–Aldrich, Korea), ammonium peroxy disulfate (Sigma–Aldrich, Korea) and hydrogen peroxide (Sigma–Aldrich, Korea) in a glass bottle at room temperature and sonicated for 3 min. Subsequently, the glass bottle was placed in a domestic microwave oven and irradiated at 500 W for 90 s [24]. Under microwave radiation, the precursors exfoliated rapidly, accompanied by lightening (caution: excessive microwave intensity or subjecting the reaction mixture to longer times or large volumes of reacting mixtures can cause violent explosions). Expanded graphene platelets, which rose on the walls of the glass bottle during microwave radiation process, were separated from the bulk graphite through ultrasonication in organic solvent medium such as acetone. The resultant solution was filtered using 0.45 μm filter paper and dried under vacuum to get graphene nanoplatelets. The synthesized graphene platelets were treated with hydrazine hydrate solution at 80 °C to reduce the oxygen moieties developed during microwave radiation process. The morphological characterizations of the GNSs were done using TEM (JEOL-2100F) and FE-SEM (LEO SUPRA 55, Carl Zeiss, Germany). The structural features of the GNSs were determined using FT-IR (Perkin-Elmer spectrophotometer), X-ray diffraction (D8 Advance, Bruker) and Raman spectroscopy (RFS-100/S, Bruker). The surface elemental composition of the synthesized GNSs was analyzed using K-Alpha X-ray photoelectron spectroscopy (XPS, Thermoelectron Inc.).

The electrochemical performances of Li-ion anode materials fabricated using GNSs were measured by fabricating 2032-type Li-ion half cells. Electrodes were prepared by casting a slurry with a composition of 90 wt.% GNSs, 5 wt.% of super P (TIMCAL) and 5 wt.% of PVDF binder (Kureha KF100) onto a copper current collector foil. The slurry was prepared by grinding the mixture in the presence of N-methyl pyrrolidone solvent using mortar for 15 min. The viscous slurry coated onto copper foil was dried in oven at 100 °C for 5 h. The dried coating electrode was pressed under a 7 t load and then punched out with size of 14 mm in diameter. The active material mass loading was 1.5 mg cm^{-2}. The electrode was assembled into 2032 type coin type cell with 1 M $LiPF_6$ solution in a 1:1 (volume) mixture of ethylene carbonate (EC) and dimethyl carbonate (DMC) (Merck Co.) as an electrolyte. Metallic lithium was used as the counter and reference electrode. Electrochemical properties of the coin type cells were galvanostatically charged and discharged in the voltage range of 0.01–3.0 V vs. Li/Li^+ using Wonatech battery analyzer. Cyclic voltammetry curves were measured at 0.1 mV s^{-1} within the range of 0.01–3 V using an electrochemical work station (CHI 660C). Electrochemical impedance studies of the Li-ion cells were performed using an electrochemical work station (CHI 660B) by applying sine wave with amplitude of 5.0 mV in the frequency range of 100 kHz to 0.01 Hz.

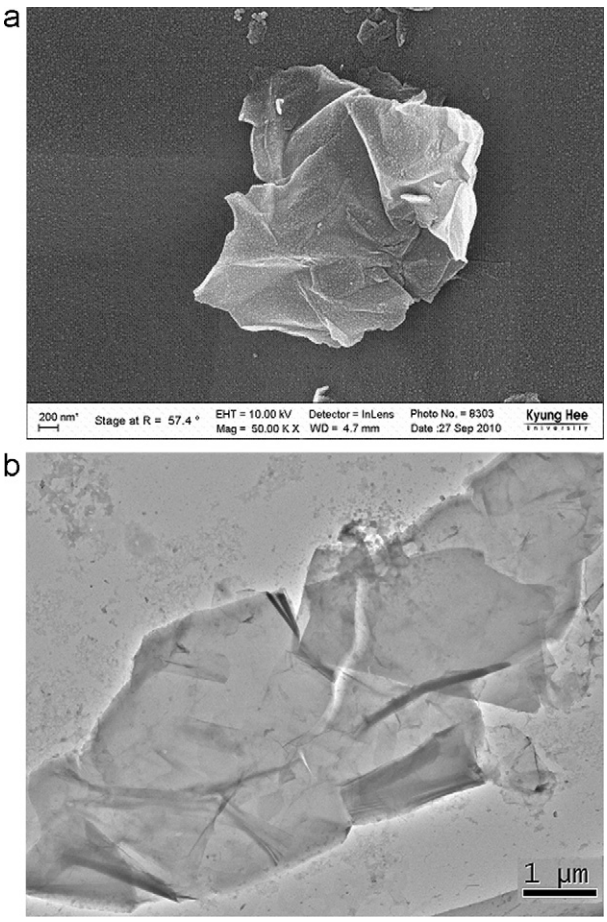

Fig. 1. (a) FE-SEM image of graphene nanosheet (b) TEM image of graphene nanosheets.

3. Results and discussion

The morphology of the graphene nanosheets (GNSs) prepared through microwave radiation is determined using FE-SEM and TEM. From FE-SEM results (Fig. 1a), it can be revealed that the GNSs consist of crumbled and curved structure that are visible in the micrometer domain. Low magnification TEM image of giant graphene nanosheets corroborates that they are scrolled and entangled with each other (Fig. 1b). Corrugation and scrolling are part of the intrinsic nature of graphene nanosheets, which results from the fact that the 2D membrane structure becomes thermodynamically stable via bending [25]. Through FE-SEM and TEM analysis, it can be understand that graphene nanosheets tend to scroll down leading to nanovoids and nanocavites in the scrolled sheets. The interplanar distance corresponding to the spacing of the (0 0 2) planes of the GNSs measured using X-ray diffraction is observed to be 0.37 nm, which is larger than that of graphite (0.34 nm) (figure not shown). The BET surface area of the GNSs prepared through microwave radiation is observed to be 590 m^2 g^{-1} and this value is significantly lower than the theoretical surface area (2200 m^2 g^{-1}) of the graphene material. This may be attributed to less nitrogen adsorption due to the overlap of the stacked layers of the exfoliated graphenes [24].

XPS survey scan results of graphene nanosheets synthesized through microwave process shows a sharp peak at 285 eV, which corresponds to the C1s peak along with the appearance of small

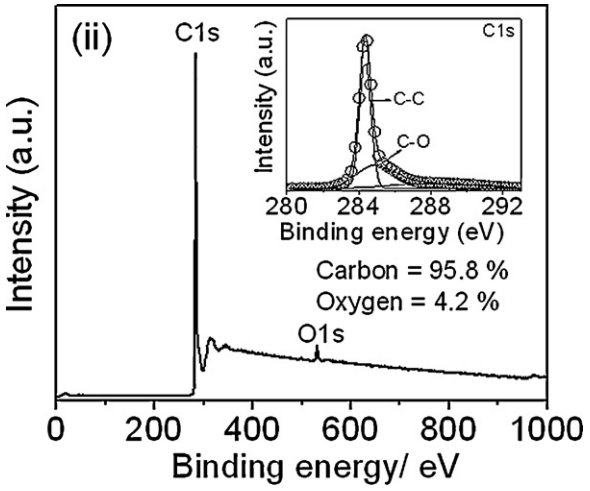

Fig. 2. XPS result of graphene (inset: high resolution C1s spectrum of graphene).

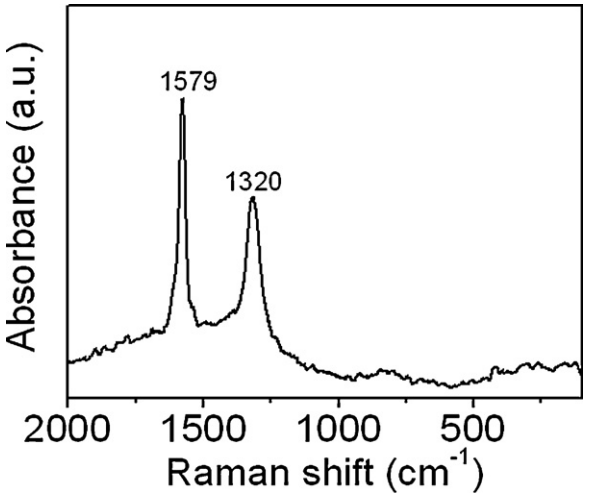

Fig. 4. Raman spectroscopic result of graphene.

peak at 530 eV corresponding to the O1s peak (Fig. 2). The carbon and oxygen atomic percentages calculated using XPS survey scan results revealed that the trace amount of oxygen functionalities presents even after hydrazine reduction. High resolution spectra of C1s peak shows three peaks that are corroborated to –C–C– (284.5 eV), C–O (285.5 eV) and π–π^* transition of carbon peak (satellite peak at 290 eV) (Fig. 2 (inset)). The FT-IR spectrum of GNSs reveals the presence of oxygen containing groups (–C=O, 1700 cm^{-1}) (Fig. 3), which is derived from the oxidation during microwave radiation. The shoulder peak at 1575 cm^{-1} may reflect the skeletal vibration of graphene nanosheets similar to expanded graphite as reported by other research groups [26].

Raman spectroscopy is a non-destructive approach to characterize graphitic materials, and in particular to determine ordered and disordered crystal structures of graphene nanosheets. Fig. 4 shows the Raman spectrum of the as-prepared graphene nanosheets. GNSs exhibits a D-band at 1320 cm^{-1}, which corresponds to a breathing mode or k-point photons of A1g symmetry, and a strong G band at 1579 cm^{-1} that should be assigned to the in-plane bond-stretching motion of pairs of C sp^2 atoms (the first order scattering of the E_{2g} photons). Compared to pure graphite, there is a blue shift in G position by 4 cm^{-1} and this shift is attributed to the transformation of the bulk graphite crystals to graphene nanosheets (figure not shown) [26]. Ogawa et al. [27] proposed a correlation between the FWHM and I_D/I_G ratio to the degree of the disorder between the inter-gallery layers and planar graphene domain size, respectively. The ratio of the D band to G band (I_D/I_G) of the microwave synthesized graphene nanosheets is about 0.7 V with almost equal full width at half height maximum (FWHM) indicating well stacked nature of graphene nanosheets (Fig. 4) [28].

The electrochemical properties of graphene nanosheets as anodes in lithium-ion cells are evaluated via constant current charge/discharge cycling in the potential range from 0.01 to 3.0 V at 0.1 C rate. The charge/discharge profiles of graphene anode in the first and the 50th cycle are shown in Fig. 5. Unlike the chemically prepared graphene-based anode materials, GNSs synthesized through microwave radiation exhibit charge/discharge profile with distinct potential plateaus. In the first cycle, the voltage plateau at about 0.7 V can be attributed to the electrolyte dissociation and the solid electrolyte interface (SEI) film formation on the electrode surface [29]. In the discharge process (lithium insertion), the slope of the curve starts from 3.0 V with the largest part of the specific capacity (>70%) falls in the region below 0.5 V. The capacity below 0.5 V could correspond to the lithium binding on the basal plane of the graphene nanosheets. While, the capacity above 0.5 V could be ascribed to the faradic capacitance on the surface or on the edge sites of graphene nanosheets. GNS anode delivered a specific capacity of 580 mAh g^{-1} in the initial discharge process and

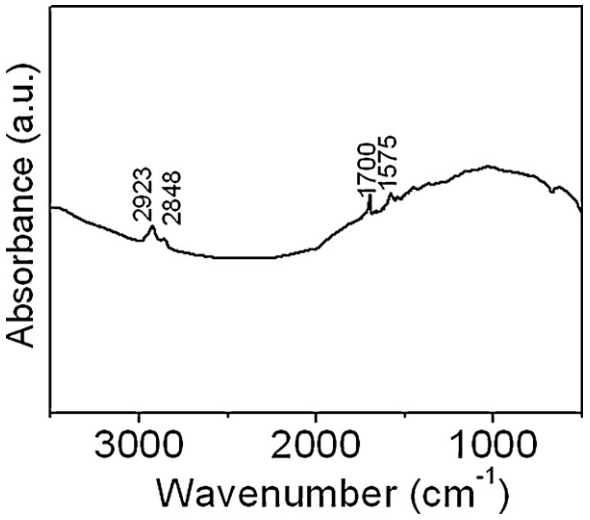

Fig. 3. FT-IR result of graphene nanosheet.

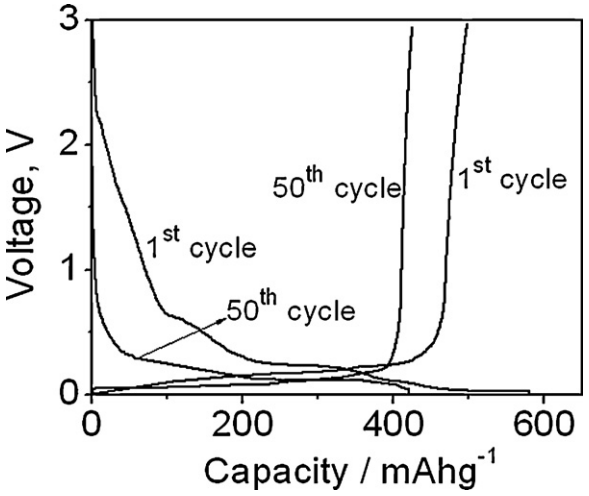

Fig. 5. Charge–discharge profiles of graphene electrodes.

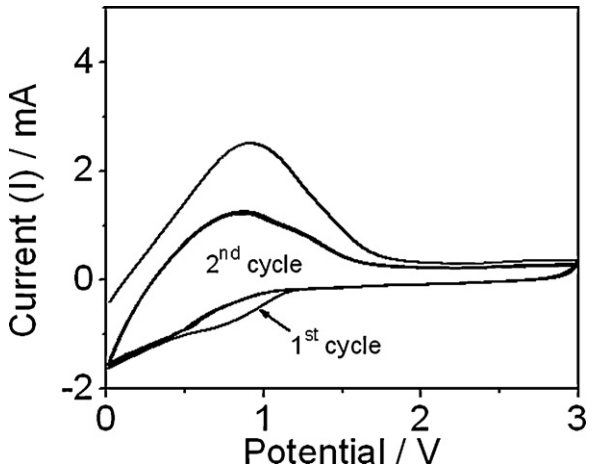

Fig. 6. Cyclic voltammogram of graphene-based anode materials.

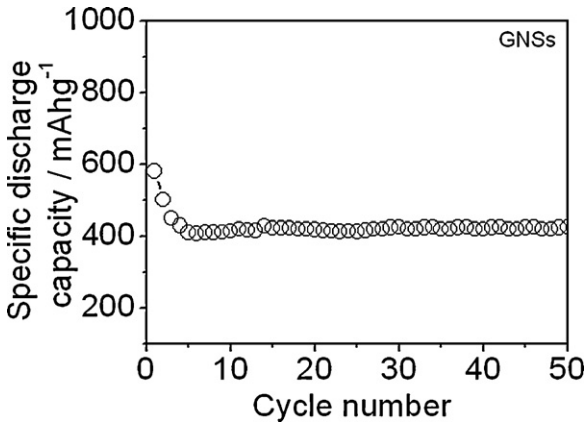

Fig. 7. Cycle performance of graphene electrodes.

a reversible capacity of 500 mAh g^{-1} in the first charging process. The reversible capacity at 50th cycle is observed to be 420 mAh g^{-1} and this value significantly higher compared to graphite anodes [30]. The higher reversible capacity of GNSs compared to graphite is ascribed to the lithium storage on both sides of graphene surface and in the micropores/nanocavites present in the GNS electrodes. According to micropore mechanism, the extraction of lithium from the nano-cavities has to go through the way of graphene crystallites. Earlier report on graphite based electrodes reveals that the graphite retains about 81% (columbic efficiency) of its initial specific discharge capacity even after 50 cycles [31]. The specific discharge capacity of the synthesized GNSs material based electrodes decreases to about 27.6% (columbic efficiency, 72.4%) in 50 cycles corroborating its irreversible nature compared to graphite electrodes though the lithium storage capacity is significantly higher for GNSs based electrodes. Slightly higher irreversible nature of GNSs compared to graphite may be attributed to the presence of residual oxygen containing functional groups in the nanopores of the graphene electrode that chemically reacts with the lithium ion resulting in the appreciable voltage hysteresis during the charging process. It is interesting to note that the charge/discharge profiles of GNSs synthesized through microwave process is quite similar to the charge/discharge profiles of oxidized graphite though the GNSs exhibits a higher discharge capacity value compared to the oxidized graphite [13]. This may be attributed to the presence of some microstructural graphite platelets along with the disorganized graphene stacks in the fabricated electrodes. It should be noted that the GNS electrodes prepared through microwave synthesis exhibit a broad electrochemical window (0–3.0 eV) as a function of the lithium capacity and the large voltage hysteresis, similar to the nongraphitic carbons [30].

The cyclic voltammograms (CV) of the graphene anode are shown in Fig. 6. The potential range is set in the range of 3.0–0.0 V at the scan rate of 0.1 mV s^{-1}. The CV profiles are almost similar to the graphite with the peak maximum occurs at around the potential of 0.7 V that corresponds to the lithium ion intercalation/deintercalation process. In contrast to the earlier reports on the CV of graphite based electrodes, microwave-assisted graphene electrodes shows a significant decrease peak position value in the subsequent cycles revealing the current loss as observed in the graphene prepared through chemical modification [31].

Cyclic performances of GNS electrode are shown in Fig. 7. The cycleability of the graphene electrodes is examined under long-term cycling over 50 cycles, which demonstrated a good cyclic performance and reversibility. After 50 cycles, the graphene electrodes still maintained a specific capacity of 420 mAh g^{-1}, which represents much enhanced electrochemical performances compared to that of graphite electrodes. Further improvements are expected by tuning the size of the individual graphene sheets and graphitic structure of the graphene sheets by adjusting the microwave processing parameters and/or introducing nanocrystals between the graphene platelets. The large irreversible capacity of the graphene electrodes is expected to be decreased by the surface modification through various methods, such as the reduction or carbonization process to remove the surface functional groups [32].

The typical Nyquist plot of AC-impedance measured after 1st and 50th cycle of GNS electrode is shown in Fig. 8. The electrochemical impedance spectrum is obtained in the frequency range of 10^{-2}–10^{5} Hz. In general, the impedance spectrum of GNSs consists of depressed arc followed by the straight line inclined at 45° angle. Earlier proposed models suggest that the distorted arc at the high frequency region consists of two semi-circles along with the inclined straight line. The first semi-circle at high frequency region is ascribed to the formation of SEI film and/or contact resistance, while the semicircle in the medium frequency region is assigned to the charge-transfer impedance on electrode/electrolyte interface, and the inclined line at an approximate 45° angle to the real axis corresponds to the lithium-ion diffusion process within carbon electrodes [33]. From the Fig. 8, it is clearly visible that the diameter of the semi-circle at the medium frequency region is reduced significantly with increasing cycle number, revealing the fact that the charge-transfer resistance decreases with cycle number. The presence of functional groups at the unorganized carbon

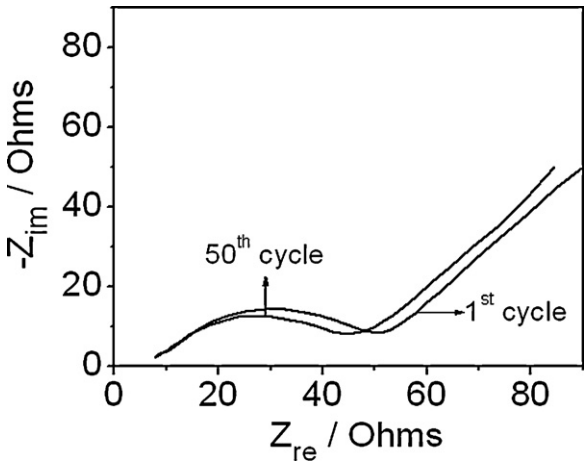

Fig. 8. AC impedance spectra of graphene electrodes.

sites results in more irreversible lithium insertion in the electrode with the growth of cycle number that leads to the increase of electrical conductivity of GNSs [34]. Decrease in charge-transfer resistance with increasing cycle number corroborates the fact that GNSs prepared through microwave process are more favorable for the lithium-ion transfer at the electrode/electrolyte interface. The exchange current density (i_0) can be calculated using the equation $i_0 = RT/nFR_{ct}$, where R is the gas constant, T is the absolute temperature, n is the number of electrons, F is the Faraday constant and R_{ct} is the charge-transfer resistance [13]. Since the charge-transfer resistance of GNS electrodes decreases with the number of charge/discharge cycles, it is expected that the exchange current density of GNSs increases implying the enhanced electrochemical activity of GNSs synthesized through microwave radiation process.

4. Conclusion

Graphene nanosheets have been prepared by the oxidation and expansion of graphite through microwave radiation process. FE-SEM observation revealed that the loose graphene nanosheets exist as crumbled and curved nanostructures. Raman spectroscopy and X-ray diffraction confirmed the graphitic crystalline structure of graphene nanosheets. Coin type cells were fabricated using the synthesized GNSs as anode and characterized for its electrochemical performances. The reversible capacity of the synthesized graphene is almost twice that the graphite, due to the storage of Li-ion on the micropores and nanovoids present in the synthesized GNSs. The exchange current density of GNS anodes increases with increasing charge/discharge cycles, corroborating the enhanced electrochemical activity of the GNSs.

Acknowledgement

This work was supported by Kyung Hee University grant in 2011 (KHU-20110187).

References

[1] J.M. Tarascon, M. Armand, Nature 414 (2001) 359.
[2] P.G. Bruce, B. Scrosati, J.M. Tarascon, Angew. Chem. Int. Ed. 47 (2008) 2930.
[3] S.H. Ng, J.Z. Wang, D. Wexler, K. Konstantinov, Z.P. Guo, H.K. Liu, Angew. Chem. Int. Ed. 45 (2006) 6896.
[4] P.A. Thrower, G.K. Mathew, N.J. McGinnis, Carbon 20 (1982) 465.
[5] E. Peled, C. Menachem, A. Melman, J. Electrochem. Soc. 143 (1996) L4.
[6] B. Henschke, R. Xchloegl, T. Schedel-Niedrig, M. Keil, N.M. Frankfurt, J. Phys. Chem. 64 (1992) 4522.
[7] S.G. Oh, R.J. Baker, J. Catal. 128 (1991) 137.
[8] Y. Wu, C. Jiang, C. Wan, E. Tsuchida, Electrochem. Commun. 2 (2000) 272.
[9] L.J. Fu, H. Liu, C. Li, Y.P. Wu, E. Rahm, R. Holze, H.Q. Wu, Solid State Sci. 8 (2006) 113.
[10] K.S. Novoselov, A.K. Geim, S.V. Morozov, D. Jiang, Y. Zhang, S.V. Dubonos, I.V. Grigorieva, A.A. Firsov, Science 306 (2004) 666.
[11] K.S. Novoselov, A.K. Geim, S.V. Morozov, D. Jiang, M.I. Katsnelson, I.V. Grigorieva, S.V. Dubonos, A.A. Firsov, Nature 438 (2005) 197.
[12] Y. Hernandez, V. Nicolosi, Nat. Nanotechnol. 3 (2008) 563.
[13] P. Guo, H. Song, X. Chen, Electrochem. Commun. 11 (2009) 1320.
[14] Y. Zhou, D. Bao, L.A.L. Tang, Y. Zhong, K.P. Loh, Chem. Mater. 21 (2009) 2950.
[15] H. Wang, H.S. Casalongue, Y. Liang, H.J. Dai, J. Am. Chem. Soc. 132 (2010) 7472.
[16] Y. Liang, D. Wu, X. Feng, K. Mullen, Adv. Mater. 21 (2009) 1679.
[17] K. Fukuda, K. Kikuya, K. Isono, M. Yoshio, J. Power Sources 69 (1997) 165.
[18] E. Yoo, J. Kim, E. Hosono, H. Zhou, T. Kudo, I. Honma, Nano Lett. 8 (2008) 2277.
[19] K. Tatsumi, N. Iwashita, H. Sakaebe, H. Shioyama, S. Higuchi, A. Mabuchi, H. Fujimoto, J. Electrochem. Soc. 142 (1995) 716.
[20] J.R. Dahn, T. Zheng, Y. Liu, J.S. Xue, Science 270 (1995) 590.
[21] S.J. Park, R.S. Ruoff, Nat. Nanotechnol. 4 (2009) 217.
[22] A. Zhamu, B.Z. Zhang, US Patent, (2009) USP 20,090,028,778.
[23] S. Vadukumpully, J. Paul, S. Valiyaveettil, Carbon 47 (2009) 3288.
[24] V. Sridhar, J.-H. Jeon, I.-K. Oh, Carbon 48 (2010) 2953.
[25] J.C. Meyer, A.K. Geim, M.I. Katsnelson, K.S. Novoselov, T.J. Booth, S. Roth, Nature 446 (2007) 60–63.
[26] M.A. Pimenta, G. Dresselhaus, M.S. Dresselhaus, L.A. Cancado, A. Jorio, R. Sato, Phys. Chem. Chem. Phys. 9 (2007) 1276.
[27] Y. Ogawa, A. Nakamura, A. Tanaka, J. Temmyo, Jpn. J. Appl. Phys. 48 (2009) 04C140.
[28] J. Yao, G.X. Wang, J.H. Ahn, H.K. Liu, S.X. Dou, J. Power Sources 114 (2003) 292.
[29] C. Wang, D. Li, C.O. Too, G.C. Wallace, Chem. Mater. 21 (2009) 2604.
[30] G.F. Ortiz, R. Alcántara, P. Lavera, J.L. Tirado, J. Electrochem. Soc. 152 (2005) A1797.
[31] G. Wang, X. Shen, J. Yao, J. Park, Carbon 47 (2009) 2049.
[32] S. Yang, H. Song, X. Chen, Electrochem. Commun. 8 (2006) 137.
[33] S. Yang, H. Song, X. Chen, A.V. Okotrub, L.G. Bulusheva, Electrochim. Acta 52 (2007) 5286.
[34] J. Giraudet, M. Dubois, J. Inacio, A. Hamwi, Carbon 41 (2003) 453.